An Online Capacitance Modeling Tool for Conductors that may be Represented as Simply-Connected Polygonal Geometries in 2.5D

F. Li* and J. V. Clark**

Purdue University, Indiana, USA, *li200@purdue.edu, **jvclark@purdue.edu
1205 W. State St., West Lafayette, IN, USA 47906

ABSTRACT

We present an online software tool that quickly and accurately calculates the capacitance of conductors that may be represented as simply-connected polygonal geometries in 2.5D with Dirichlet boundary conditions. We achieve numerical accuracy of the tool by using Schwarz-Christoffel mapping (SCM) which treats the fringing fields at vertices exactly. Our tool compares favorably in both accuracy and speed to the results found by 2.5D finite element analysis (FEA). For a test case, we model and simulate a MEMS cantilever model. We find that our tool computes capacitance about 1000 times faster than traditional FEA.

Keywords: Schwarz-Christoffel mapping, electrostatics modeling, capacitance

1 INTRODUCTION

Electrostatic sensing and actuation mechanisms are widely used in various micro-electro-mechanical systems (MEMS). For increased productivity, it is advantageous to be able to quickly and accurately compute the capacitance of the various geometric configurations in designing or investigating the behavior of MEMS. The analytical parallel-plate approximation method has been widely used to calculate capacitances [1]. The approximation is good for finite parallel plates with a gap much smaller than the length or width of the plate, but the approximation becomes inaccurate for configurations that diverge from this. Distributed element analysis tools become accurate once convergence analysis is performed, where the results of successive simulations of mesh refinement are compared until a desired tolerance level is achieved. Schwarz-Christoffel mapping methods (SCM) have previously been used in MEMS [2], [3] to find capacitance with excellent results. In these efforts, SCM has only been applied to MEMS devices with of a limited set of specific geometries. However, we have theoretically proven that SCM can be used for determining the capacitance of arbitrary simply-connected 2.5D geometry in [4].

To allow researchers to investigate a much larger set of MEMS geometries using the SCM method, we present an online software tool that quickly and accurately models and simulates the capacitance of MEMS that can be represented as simply-connected geometries in 2.5D with Dirichlet boundary conditions. The benefit of using the SCM is that it treats fringing fields at vertices exactly, which distributed element analyses methods (e.g. finite and boundary element methods) are not able to do. However, the SCM is limited to 2.5D. Distributed element analyses are usually required for 3D configurations that cannot be adequately reduced to 2.5D. By 2.5D, we mean 2D geometry that is extruded out of plane in the 3rd dimension.

The rest of the paper is organized as follows. In Section 2, we provide the details of the Schwarz-Christoffel mapping that is used in the SCM too and how we extend the results of this mapping to determine the capacitance for arbitrary 2.5D geometries. We apply SCM to a torsional actuator and compare our results with against those obtained by both analytical and finite element analysis. We summarize our conclusion in Section 3.

2 THEORY

In this section, we present the theoretical basis behind our SCM method with a MEMS torsional actuator as a test case.

2.1 Schwarz-Christoffel mapping (SCM)

We use a freely available numerical SCM toolbox [5] written in MATLAB [6] to map a physical domain (*Z*-plane) onto an ideal infinite parallel-plate domain (*W*-plane) as shown in Figure 1. In Figure 1a, we show an arbitrary simply-connected 2D geometry in the physical *Z*-plane with five vertices, where vertices z_3 and z_5 are located at infinity. Other simply-connected geometries and numbers of vertices are possible. The geometry has two Dirichlet boundary conditions: the upper and the lower boundaries at constant potentials V_1 and V_2, respectively. We choose to map the domain defined by these five vertices onto a strip domain in a *W*-plane. See Figure 1b. The two *W*-plane boundaries of the strip domain have the same potentials as those in the physical *Z*-plane domain. In the *W*-plane, the vertices z_i are mapped to the so-called prevertics w_i. We select the strip domain because it represents a true infinite parallel-plate. I.e., the exact capacitance in the *W*-plane is

$$C = \frac{\varepsilon h |w_1 - w_2|}{g}, \qquad (1)$$

where ε is the permittivity of the medium between the boundaries, $|w_1 - w_2|$ is the distance between prevertices w_1 and w_2, h is the out-of-plane thickness of the strip domain, and g is the distance between the two boundaries of the strip domain which is a unit.

The capacitance of the boundary portion between w_1 and w_2 in the *W*-plane is exactly the same as that between vertices z_1 and z_2 in *Z*-plane. However, the electric field lines in the red cross-hatched area in the *W*-plane are horizontal and evenly spaced, and the electric field lines in the *Z*-plane are nonlinear, uneven, and subject to fringing.

2.2 Torsional actuator: analytical

In this section we formulate the approximate capacitance of a torsional actuator, which we later compare to the results of our SCM tool. We show a schematic of the MEMS torsional actuator in Figure 2a. The upper plate is the proof mass with length L, cross sectional thickness *t*, and out-of-xy-plane dimension h. The proof mass is suspended by torsional flexures. The substrate is grounded, while an actuation voltage, V, is applied on the proof mass. The dimensions of the substrate in both x and z directions are much larger than the length L and width h of the proof mass. The initial distance between the proof mass and the substrate is g. Upon actuation, the proof mass rotates a small angle θ about the torsional flexures and towards the bottom electrode as shown in Figure 2b.

The capacitance of a small element shown by the dashed lines in Figure 2b is commonly approximated as [7]-[10]

$$dC = \frac{\varepsilon\, dA}{g(x)} = \frac{\varepsilon w\, dx}{g - x\tan\theta}. \qquad (2)$$

Because θ is small, $\tan\theta$ approximately equals θ. Equation (2) becomes

$$dC = \frac{\varepsilon w\, dx}{g - x\theta}. \qquad (3)$$

By integrating (3) along the length of the proof mass, the total capacitance of the torsional actuator is about

$$C = \int_0^L \frac{\varepsilon w\, dx}{g - x\theta} = \frac{\varepsilon w}{\theta} \ln\frac{g}{g - L\theta}. \qquad (4)$$

2.3 Torsional actuator: SCM

To compare SCM with the analytical formulation in (4), we choose the following geometric configuration for the

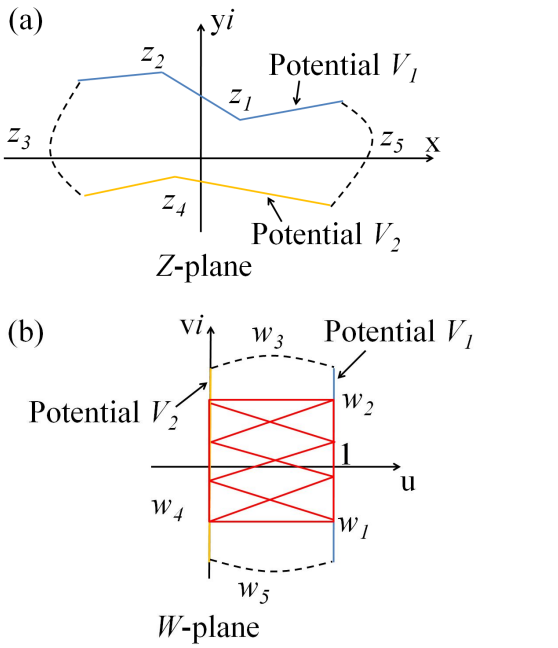

Figure 1: Illustration of SCM planes. A simply-connected 2.5D geometry in a physical *Z*-plane with five vertices (z_3 and z_5 are located at infinity.) is show in (a). The two boundaries have potential V_1 and V_2. Using SCM, the *Z*-plane can be mapped onto a strip domain in the *W*-plane, which is shown in (b). I.e. each z_j is mapped to w_j.

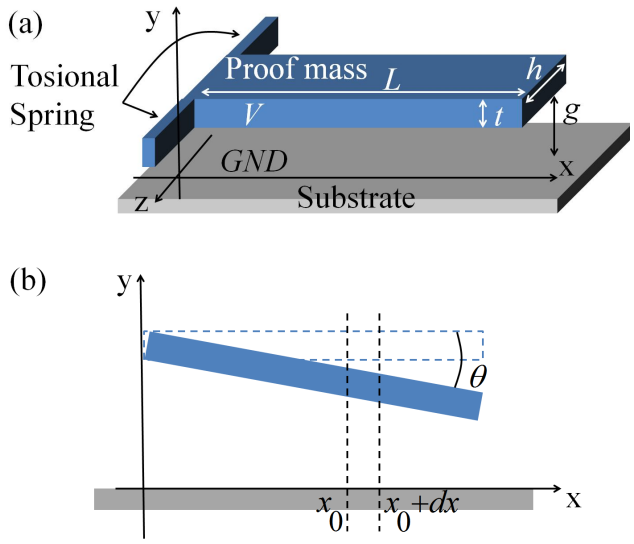

Figure 2: MEMS torsional actuator model. The 3D MEMS torsional actuator is shown in (a). The length, width, and out of plane thickness of the proof mass is *L*, *t*, and *h*. The dimensions of the substrate in both x and z directions are much larger than the length and width of the proof mass. The initial gap between the proof mass and the electrode is *g*. The proof mass rotates by a small angle θ when actuated as shown in (b).

torsional actuator: $\theta = 0.04rad$, $L = 10\mu m$, $t = 0.6\mu m$, and $g = 1\mu m$. In Figure 3 we show the electric field lines generated by the SCM. To represent the torsional actuator in the SCM tool as simply-connected polygon, we have the middle boundary on the top surface of the actuator go up to infinity. This detour from the regular geometry is small in significance because very little charge resides in the middle on the top surface (verified below). The analytical formula

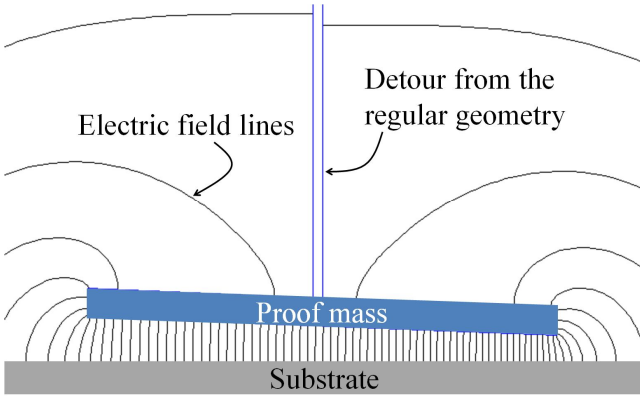

Figure 3: SCM method for simulating the MEMS torsional actuator. The sketch of the model in the SCM tool is shown. In order to make the model simply-connected, we break the top surface of the proof mass. We show the electric field lines generated by SCM tool when $\theta = 0.04[rad]$.

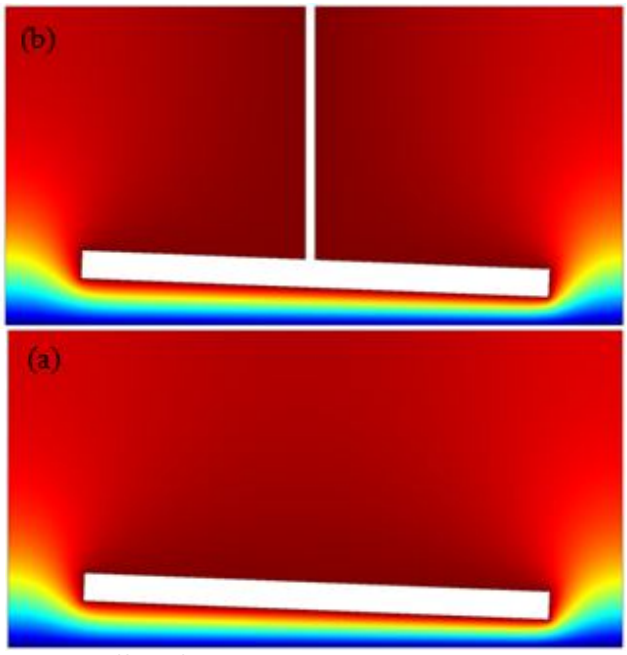

Figure 4: Effect of the boundary detour using FEA. 2.5D cross section of the torsional actuator with a boundary detour (a) and without a detour (b). The relative error of the capacitance between the 2 configurations is 0.03%. This evidence supports our use of the detour in our SCM model. The potential field is plotted, where the torsional plate and boundary detour are at a finite potential, the substrate is grounded, and the other boundaries are zero charge symmetry.

in (4) completely ignores the side and top surfaces of the torsional actuator. However, SCM accurately accounts for the side and top surfaces near the ends of the plate, which have significant fringing fields. The prevertices w_j in the *W*-planes are provided by SCM tool numerically. The capacitance of any boundary between two points in the *W*-plane can be calculated by (1) after calculating the prevertices of those two points in the *Z*-pane.

As expected, the capacitance found by the SCM method is larger than the capacitance found using (4). At a deflection of 0.04 *rad* for the configuration given in Figure 2, the absolute relative error between the SCM and analytical method is 18.23%.

2.4 Torsional actuator: FEA

The analytical formula (4) ignores the fringing fields and top surface charges. In this section we compare our SCM method with a distributed element analysis tool that is able to account for such phenomena.

For our distributed element analysis, we use the FEA software package COMSOL 3.5a [11] and use the same geometry that we use in the previous sections for the torsional actuator, and treat it as a perfect conductor.

First, to find out if the boundary detour taken with the SCM method is insignificant, we use FEA to compare the torsional actuator with and without the boundary detour (see Figures 4a and 4b). Our FEA simulation results indicate that difference between the two configurations is only 0.03%, which affects the 4th significant digit in capacitance result, where we use ~7200 meshed elements.

In comparing these capacitance results with SCM, FEA is 3.7% larger than SCM. We find that the capacitance results in FEA is greatly affected by the size of its universe, boundary conditions, and mesh density, and element type. That is, in SCM the universe is infinite, versus finite in FEA, which affects the potential gradients and therefore actuator's capacity to store charge. And the FEA boundary condition zero charge / symmetry is close but not the same as a boundary positioned at infinity in SCM. We chose linear mesh elements and a mesh density that was refined multiple times in FEA. Regarding time, for an FEA universe that is 10 times larger than the length of the actuator, and an FEA convergence tolerance of 0.1%, FEA took 1000 times as long as our 2-second SCM computation.

Due to the slight differences between the boundary conditions between SCM and FEA in modeling the torsional actuator, we perform analysis on a configuration that can be more identically applied to both analyses. In Figure 5 we show our verification results. Here, the center cantilever is at a finite potential; the top, left, and bottom boundaries are grounded; and the right-most boundaries are at infinity for SCM, and zero charge / symmetry for FEA. Although the right-most boundary conditions are slightly different, the equipotentials are very much alike. The relative error in capacitance is 0.4%, an order of magnitude better than the previous analysis between Figures 3 and 4.

3 CONCLUSION

In this paper we presented an online software tool that quickly and accurately calculates the capacitance of conductors that may be represented as simply-connected polygonal geometries in 2.5D with Dirichlet boundary conditions. We achieved numerical accuracy of the tool by using Schwarz-Christoffel mapping (SCM) which treats the fringing fields at vertices exactly. Compared to previous efforts using the SCM, our tools is able to determine the capacitance of a much larger variety of geometries. However, our SCM method is limited to simply-connected geometries in 2.5D. We found that by strategically modifying the original geometry on boundaries with the least amount of charge, we are able to obtain good results as verified by finite element analysis (FEA). Our tool compares favorably in accuracy to analytical methods, and favorably in both accuracy and speed to the results found by 2.5D FEA. Using a torsional actuator as a test case, we find that our SCM tool is about 1000 times faster than FEA.

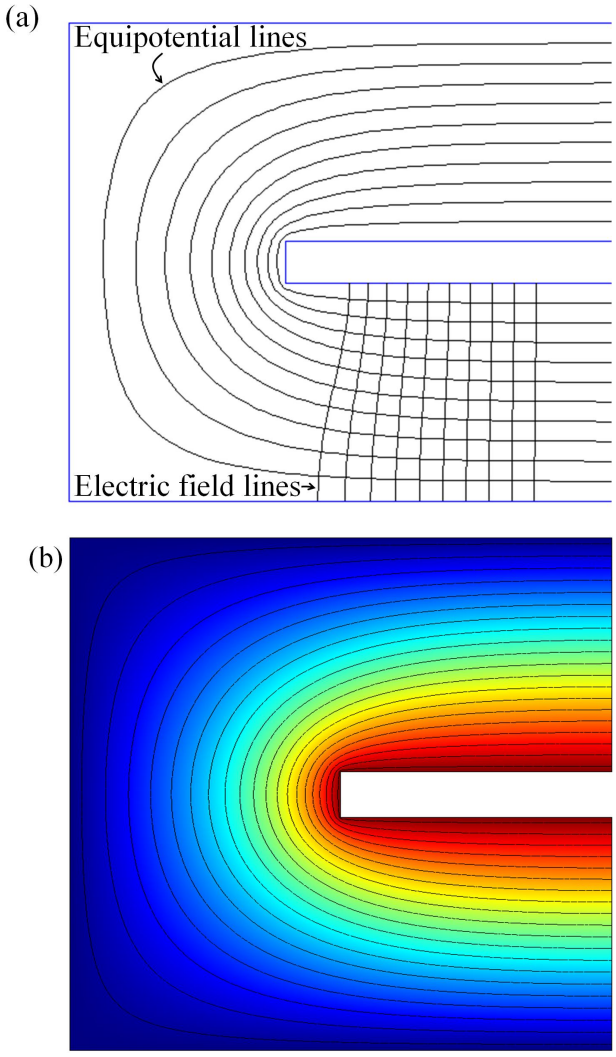

Figure 5: SCM vs FEA for nearly identical boundary conditions. The center cantilever is at a finite potential; the top, left, and bottom boundaries are grounded; and the right-most boundaries are at infinity for SCM and zero charge / symmetry for FEA. The relative error between the two capacitance simulations is 0.04%.

ACKNOWLEDGEMENT

The authors would like to thank T. Driscoll for insightful discussions about his SCM tool. This work is sponsored in by the NSF-supported NanoHUB / Network for Computational Nanotechnology and Cyber Enabled Discovery and Innovation.

REFERENCES

[1] N. van Der Meijs and J. Fokkema, "VLSI circuit reconstruction from mask topology," *VLSI Journal*, 1984.

[2] P. Bruschi, A. Nannini, F. Pieri, G. Raffa, B. Vigna, and S. Zerbini, "Electrostatic analysis of a comb-finger actuator with Schwarz–Christoffel conformal mapping," Sensors and Actuators A: Physical, vol. 113, 2004, pp. 106-117.

[3] S. He and R.B. Mrad, "Design, Modeling, and Demonstration of a MEMS Repulsive-Force Out-of-Plane Electrostatic Micro Actuator," Journal of Microelectromechanical Systems, vol. 17, 2008, pp. 532-547.

[4] J. V. Clark, *Electro Micro Metrology*, Ph.D. Dissertation, University of California Berkeley (2005).

[5] T. A. Driscoll and L. N. Trefethen, Schwarz-Christoffel Mapping, Cambridge University Press (2002), www.math.udel.edu/~driscoll/SC/.

[6] The MathWorks, Inc. 3 Apple Hill Drive, Natick, MA, 01760. http://www.mathworks.com/.

[7] P. F. van Kessel, L. J. Hornbeck, R. E. Meier, and M. R. Douglass, .A MEMS-based projection display,. Proc. IEEE, vol. 86, no. 8, pp. 1687- 1704, 1998.

[8] J. E. Ford, V. A. Aksyuk, David J. Bishop, and J. A. Walker, .Wavelength add.drop switching using tilting micromirrors,. J. Light. Technol., vol. 17, pp. 904-911, 1999.

[9] L. Fan and M. C. Wu, .Two-dimensional optical scanner with large angular rotation realized by self-assembled micro-elevator,. Proc. IEEE LEOS Summer Topical Meeting on Optical MEMS, Monterey, Aug. 20.22, 1998, Paper WB4.

[10] J. Cheng, J. Zhe, and X. Wu, "Analytical and finite element model pull-in study of rigid and deformable electrostatic microactuators," Journal of Micromechanics and Microengineering, vol. 14, 2004, pp. 57-68.

[11] COMSOL, Inc. 1100 Glendon Avenue 17th Floor, Los Angeles, CA, 90024. http://www.comsol.com.